Rare Metal Materials and Engineering
Volume 50, Issue 8, August 2021
Available online at www.rmme.ac.cn

Science Press

Cite this article as: Chen Xi, Zhang Zhao, Xie Faqin, et al. Microstructure Evolution and Mechanical Properties of Linear Friction Welded TiAl Alloy Joint with Online Stress Relieving[J]. Rare Metal Materials and Engineering, 2021, 50(08): 2765-2770.

ARTICLE

Microstructure Evolution and Mechanical Properties of Linear Friction Welded TiAl Alloy Joint with Online Stress Relieving

Chen Xi[1], Zhang Zhao[1], Xie Faqin[1], Ma Tiejun[2], Li Wenya[2], Wu Xiangqing[1]

[1] School of Civil Aviation, Northwestern Polytechnical University, Xi'an 710072, China; [2] State Key Laboratory of Solidification Processing, Shaanxi Key Laboratory of Friction Welding Technologies, School of Materials Science and Engineering, Northwestern Polytechnical University, Xi'an 710072, China

Abstract: Crack-free TiAl joints were welded by linear friction welding with online stress relieving process. Microstructural examination demonstrates that the joint has a clearly identified weld zone which consists mainly of equiaxed γ grains with a few α_2 phase. Lamellar grains in thermo-mechanically affected zones near the weld margin are oriented along with the flow direction of the plasticized material. The microhardness of the joint presents a global increase from the base metal to the weld interface by about 1700 MPa; the tensile strength of the joints ranges from 683 MPa to 717 MPa at ambient temperature, which is comparable to that of the base metal. The refinement strengthening contributes to enhancing the joint strength.

Key words: linear friction welding; TiAl alloys; online stress relieving; microstructure; mechanical property

TiAl-based intermetallic alloy, a new class of advanced lightweight high-temperature structural material, is suitable to be used around 700~1000 °C[1,2]. It has attracted widespread attention for potential application in turbine blades of aircraft engine due to its high specific strength, excellent oxidation resistance, high specific modulus, good creep resistance and high temperature mechanical properties. TiAl-based alloys have been applied in manufacturing turbine blades of advanced aircraft engines produced by GE[3-5]. In traditional gas turbines, blades are assembled at disks applying a fir-tree arrangement. However, the fir-tree blade-disk assembly is a costly and time-consuming process[6]. In addition, fretting fatigue damage, leakage flow caused by the slotted blade to disk assembly and the large mass of the components restrict the development of high thrust-weight ratio aeroengines[7]. Because of the increasing needs to manufacture blisks (integrally bladed disks) which have lower mass, improved product quality and ease of maintenance over existing conventional slotted blade/disk assemblies, a substitution of this mechanical joining technique, linear friction welding (LFW), has been introduced[8,9].

LFW as a rather new process aiming at extending the current applications for rotary friction welding to non-axisymmetric components such as blades and disks, has attracted more and more attention due to its outstanding characteristics such as high reliability, low cost, refined microstructure and almost no weld defects[10]. In LFW, a metallurgically sound solid state joint is usually formed with the help of frictional heat generated from the reciprocating movement of one component (as the oscillation side) relative to another (as the extrusion side) under an axial force. Typical solidification defects, such as pores, pinholes, shrinkage cracks, segregation, grain coarsening and cast structure can be avoided by the absence of a liquid phase during LFW. LFW has already been widely used to join a range of materials including steel, aluminum, copper, nickel-based superalloys and titanium alloys[11-20].

To date, although LFW is of great attraction for

Received date: August 13, 2020
Foundation item: National Natural Science Foundation of China (51675435); Natural Science Fund to Basic Research in Key Areas of Shaanxi Province (2018JZ5004)
Corresponding author: Chen Xi, Ph. D., Assistant Professor, School of Civil Aviation, Northwestern Polytechnical University, Xi'an 710072, P. R. China, Tel: 0086-29-88460937, E-mail: chenxb@nwpu.edu.cn

manufacturing blisks with TiAl-based alloys, research on LFW of TiAl-based alloys is rare. Threadgill[21] in The Welding Institute (TWI) mentioned the prospects of LFW for joining dissimilar TiAl/Ti_3Al alloys; low ductility of base metal, high welding residual stress and fast cooling rate after welding will contribute to the initiation of cracks on weld interface, and further study of microstructural evolution and mechanical properties of LFWed TiAl alloys is not satisfying. There have been some researches on rotating friction welding between TiAl-based alloys and steels. According to Lee, rotating friction welded joints between TiAl alloy and AISI 4140 were achieved using Cu as insert layer[22]. Dong et al have reported the rotating friction welding of dissimilar TiAl/40Cr[23] and TiAl/42CrMo[24] joints. The results show that the as-welded specimens are failed through the interface, while the heat-treated specimens are failed on TiAl alloy side, indicating that PWHT is necessary to improve the joint strength. Therefore, due to the intrinsic properties such as brittleness and low ductility, it is indispensable to use inset layer or post-weld heat treatment (PWHT) to relive high residual stress and to avoid weld crack in TiAl joint.

To sum up, cracks are easily formed at the interface after welding due to the high residual stress and fast cooling rate, which lead to the deterioration of joint strength. It is still a challenge to achieve satisfactory TiAl joints by direct welding. Therefore, for the sake of integrity of joint, the online stress relieving process by induction heating was employed after linear friction welding immediately in this study. Microstructural examination and mechanical properties tests were carried out to examine the welding quality.

1 Experiment

The welding experiments were carried out using the LFW machine (XMH-160) developed by Northwestern Polytechnical University (China). The as-extruded TiAl alloy was used for linear friction welding and its nominal chemical composition is given in Table 1. The microstructure revealed by scanning electron microscope (SEM) shows a typical lamellar γ structure, as shown in Fig. 1. Specimens were cut into the following dimensions: width of 10 mm, length of 17 mm and height of 40 mm, while the welding interface had dimensions of 170 mm^2.

On the basis of preliminary experiments and characteristics of XMH-160, the welding parameters were selected as follows: amplitude of oscillation of 2.5 mm, frequency of oscillation of 30 Hz, friction pressure of 60 MPa and friction time of 4 s. Prior to welding, the welding surface of the samples was ground and cleaned in an acetone bath. The online stress relieving device (induction heating coil around the joint) employed in this study is shown in Fig.2, which was used immediately after welding.

Table 1 Nominal chemical composition of the TiAl alloy (wt%)

Al	Cr	V	Ni	O	N	H	Ti
31.86	1.32	3.27	0.45	0.047	0.0079	0.0008	Bal.

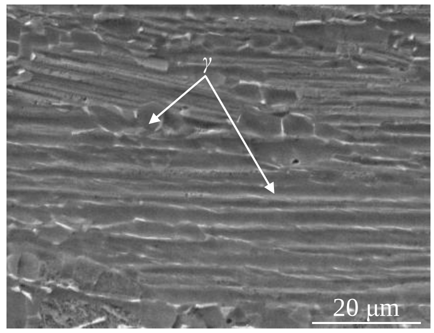

Fig.1 Microstructure of parent TiAl alloy

The joint was cut into two parts along the direction of oscillation, as demonstrated in Fig. 3, one part was used for metallurgical examination, and the other part was used for tensile strength testing which was carried out at ambient temperature according to GB/6397-86 (China). The polished metallographic specimens were etched with a solution of 10 mL HF, 30 mL HNO_3 and 70 mL H_2O. The microstructure was examined by optical microscope (OM, Olympus PMG3) and SEM (Tescan MIRA3 XMU). The tensile test was conducted at ambient temperature using a universal testing machine (Shimadzu AG-X) with a cross-head speed of 1 mm/min. The microhardness was measured along the length direction from base metal to weld line with a hardness tester (model: Duramin-A300, 500 g load). Three test lines were adopted and an average profile was obtained disregarding doubtful values.

2 Results and Discussion

2.1 Appearance of joint

As shown in Fig.4, the morphology of flash of LFWed TiAl joint is different from that of LFWed Ti joint, which can be divided into two parts: the upper flash and the lower flash[8,18-20]. The two layers of flash are not mutually adhesive and the surface has metallic luster, which is similar to that of Ni-based superalloy[15,16]. The quantity of the extruded flash of the joint is much fewer compared with that of Ti LFWed joint. As the flash layer consists of plastically deformed material

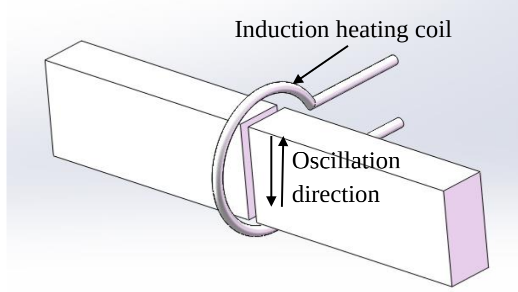

Fig.2 Online stress relieving device

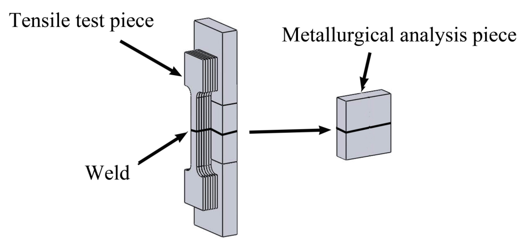

Fig.3 Metallographic specimen cut from welded specimens and dimension of tensile specimen

Fig.4 Typical post-weld LFWed TiAl joints

extruded during the welding process, the difference in the high-temperature strength between TiAl alloys and Ti alloys is almost certainly responsible for the difference in flash morphology[25].

2.2 Joint microstructure

Fig. 5a shows an overall view of the cross-sectional microstructure of the joint along the direction of oscillation. The narrow weld zone (<500 μm in width) can be clearly identified. No weld cracks are observed at weld interface, indicating that online stress relieving process used in this study is feasible to eliminate the weld cracks caused by high weld residual stress and fast cooling rate. On both sides of the joint, the orientations of γ grains near the weld zone have changed appreciably because of the oscillation and friction pressure during the welding process, which shows the flow direction of the plasticized material.

Typical microstructures in different locations (zone A, B and C) of the thermo mechanical affected zone (TMAZ) are shown in Fig. 5b~5d, respectively. Compared to the base metal, zones A, B and C possess more equiaxed grains. And the closer to the weld zone, the more lamellar structures are transformed to equiaxed structures. Zone D presents the weld center zone, as shown in Fig. 5d, in which all the lamellar structures are transformed to equiaxed grains.

The microstructure at high magnification of weld zone is illustrated in Fig. 6a, where faint indications of grain boundaries can be observed, indicating that grains in this area are not effectively revealed through chemical etching. The low etching response is ascribed to great deformation and dynamic recrystallization happening in weld zone. A few more equiaxed grains are visible in the area adjacent to weld zone as shown in Fig. 6b. Fig. 6c represents the microstructure at about 0.6 mm from the weld line, and acicular and equiaxed structures can be revealed. Finally, from the micrograph of Fig. 6d, 1.2 mm from the weld line, more lamellar structures

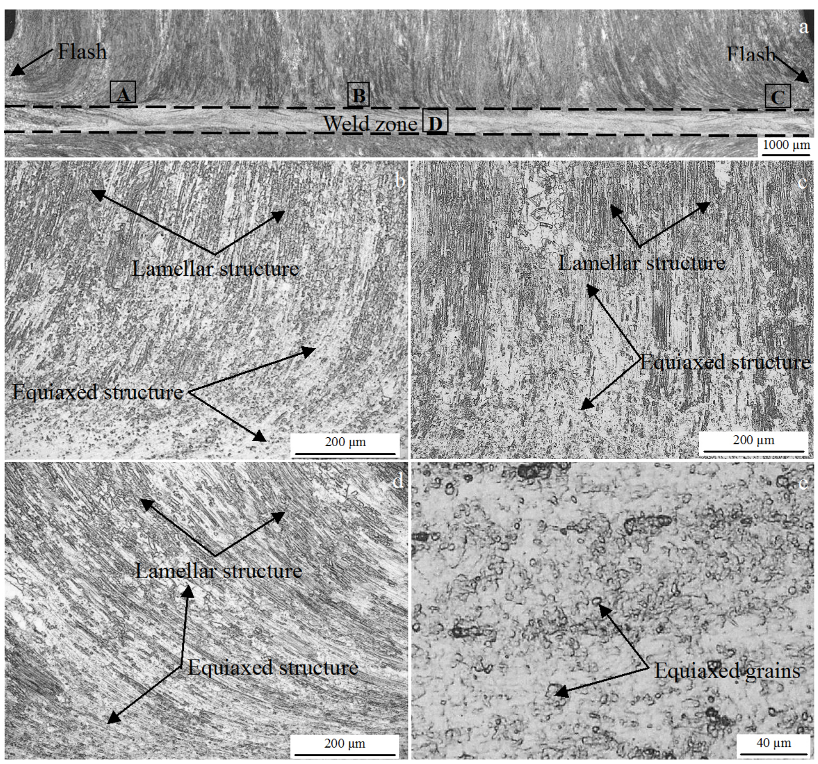

Fig.5 Typical OM microstructures of the joint: (a) overall view of the joint; (b) zone A; (c) zone B; (d) zone C; (e) weld zone

similar to the base metal (Fig. 1) can be found clearly. This characteristic of weld microstructure is also found in a LFWed near-β Ti joint[26].

In order to reveal the details of the weld zone, including the grain characteristics and phase composition, EBSD technique was performed on this area, as shown in Fig.7. Fig.7a presents the grain misorientation angle map: black and red lines represent the high-angle grain boundaries (HGBs, >15°) and low-angle grain boundaries (LGBs, 2°~15°), respectively. Equiaxed refined grains around 10 μm can be found in weld zone. As shown in Fig. 7b, the weld zone features primary HGBs with number percentage of 91.4%, revealing that weld zone undergoes complete dynamic recrystallization under the thermomechanical conditions during linear friction welding process. It has been reported that hot working above the eutectoid temperature (above 1125 °C) can totally transform the lamellar structure in TiAl alloy to equiaxed grains due to dynamic recrystallization[27,28]. Generally, the peak value of the interface temperature can easily overtake 1100 °C and reach 1200 °C during linear friction welding process[29]. In addition, the combination of elevated temperatures and high strain rates also promote the dynamic recrystallization during the LFW process. Thus, it is reasonable for the transformation from lamellar structures to equiaxed structures in weld zone. Nevertheless, in TMAZ, the temperature of TMAZ adjacent to weld zone is around the eutectoid temperature so some lamellar microstructures turn into equiaxed microstructures. But along with away from the weld zone, the effect of elevated temperature and high strain rates on microstructure in TMAZ decreases, so the lamellar structures change little.

The phase composition of weld zone is shown in Fig. 7c, where the α_2 phase and γ phase are indicated by red and blue color, respectively. It is seen that the weld zone is mainly composed of γ phase while the quantity of α_2 phase is small. It should be noted that no retained α phase is found. For TiAl alloys, when the hot working temperature enters the α+γ phase

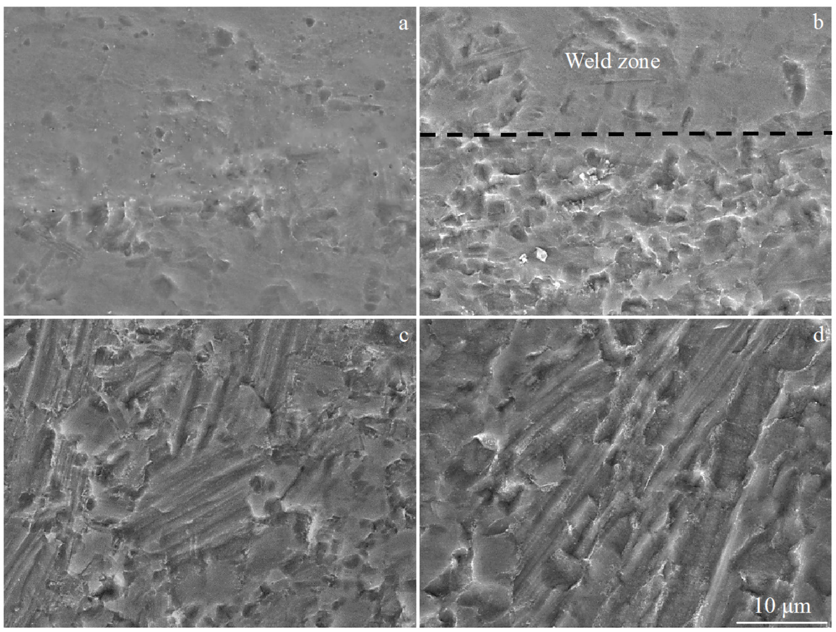

Fig.6 SEM microstructures of the joint: (a) weld zone, (b) 200 μm from weld line, (c) 600 μm from weld line, and (d) 1.2 mm from weld line

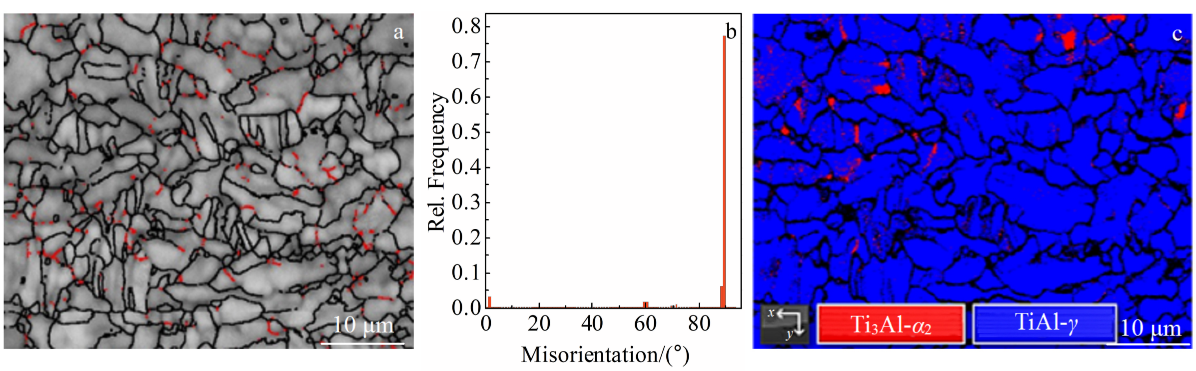

Fig.7 EBSD maps of weld zone: (a) grain boundary misorientation angle, (b) misorientation distribution and (c) phase composition

region and the cooling rate is faster than 250 K/s, a portion of α phase can remain in the alloy and develop into Widmanstatten structure due to insufficient decomposition[23,30]. In this experiment, the peak value of temperature is supposed to be above the $\alpha+\gamma$ phase transition line, and the cooling rate of LFW is about 350~400 K/s, faster than the critical cooling rate of 250 K/s[29, 31]. Thus, it is supposed that the weld zone should consist of some retained α phases. However, the online stress relieving process used after welding can offer more time for the transformation from α to $\alpha_2+\gamma$ phase. As a result, the high-temperature α phase in the weld zone fully decomposes into the γ and α_2 phase[32].

2.3 Mechanical properties

Fig. 8 presents the microhardness profile obtained for welded sample with online stress relieving. It shows the variation of microhardness from the base metal to the weld line on both oscillation side and extrusion side. The curves of both oscillation side and extrusion side have the same variation trend, and an overall increase of strength from base metal (around 3100 MPa) to weld zone (around 4800 MPa) is observed. As mentioned above, the equiaxed microstructure formed during dynamic recrystallization in weld zone contributes to improve the microhardness by refined grain strengthening.

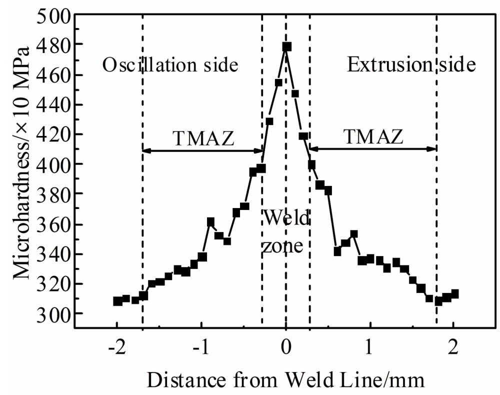

Fig.8 Distribution of microhardness across joint interface from oscillation side to extrusion side

Table 2 Tensile properties of joints at ambient temperature

Sample	UTS/MPa	YS/MPa	Elongation/%	Failed location
1	702	663	0.39	Base metal
2	717	680	0.37	Base metal
3	683	629	0.32	TMAZ

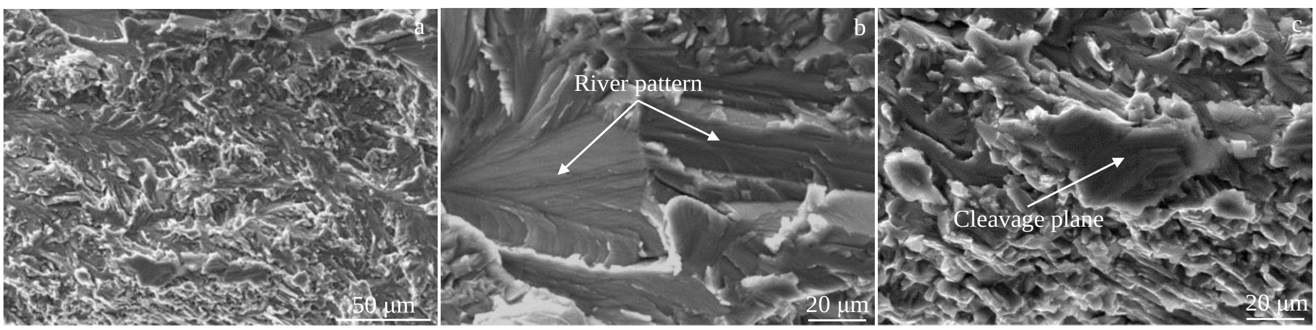

Fig.9 SEM fractographs of the joint after tensile test at ambient temperature: (a) over view, (b) river pattern and (c) cleavage plane

The tensile properties at ambient temperature of the joint are shown in Table 2. The fracture locations of sample 1 and sample 2 are far away from the weld line in the base metal area, which indicates that the tensile property of the weld is at least comparable to that of the base metal. The sound tensile strength of the welded samples can be explained by the presence of a hardened region in the weldment with a refined microstructure. However, sample 3 fails in TMAZ, while its tensile strength is comparable to that of sample 1 (702 MPa) and sample 2 (717 MPa). Sample 3 was cut from the edge of the joint, where lamellar structures in TMAZ adjacent to weld zone are nearly parallel to the plastic flow direction, as shown in Fig. 5d. It will cause the degradation of the tensile strength of the sample and result in the fracture in TMAZ[23]. The average tensile strength of the three tensile samples at ambient temperature is about 694 MPa, with the elongation of 0.35%. The corresponding fracture morphology of sample 3 exhibits quasicleavage fracture pattern, as shown in Fig. 9a. The morphology of fracture sample is composed of cleavage planes and river pattern, as shown in Fig.9b and 9c, revealing the low ductility of TiAl alloy at ambient temperature.

3 Conclusions

1) The sound linear friction welding (LFW) joints free of cracks and pores can be obtained for TiAl alloy by online stress relieving process. Microstructure examination of weld zone and TMAZ presents different features. The orientation of lamellar structure changes drastically and is parallel to the flow direction of the plasticized material formed in thermo mechanical affected zone (TMAZ) near the weld margin.

2) In the weld zone, equiaxed refined grains form due to the interaction of elevated temperatures and high strain rates during the welding process. The closer to the weld zone, the more lamellar microstructures in TMAZs are transformed into equiaxed structure. The weld zone consists mainly of γ phase

with a small portion of α_2 phase.

3) The microhardness presents an overall decrease from the interface to base metal. This trend is in accordance with the microstructural evolution. The tensile strength of the joints ranges from 683 MPa to 717 MPa at ambient temperature, which is comparable to that of the base metal. Only one specimen fails at the TMAZ due to the orientations of lamellar structure near the weld zone. The fracture morphology exhibits a quasi-cleavage pattern.

References

1 Wu Yulun, Hu Rui, Yang Jieren. *Journal of Alloys and Compounds*[J], 2019, 790: 42

2 Song Y L, Dou Z H, Zhang T A *et al*. *Journal of Alloys and Compounds*[J], 2019, 789: 266

3 Eylon D, Keller M M, Jones P E. *Intermetallics*[J], 1998, 6(7-8): 135

4 Saari H, Beddoes J, Seo D Y *et al*. *Intermetallics*[J], 2005, 13(9): 937

5 Peng Zichao, Tian Gaofeng, Jiang Jun *et al*. *Materials Science & Engineering A*[J], 2016, 676: 441

6 Aschenbruck J, Adamczuk R, Seume J R. *Procedia CIRP*[J], 2014, 22: 256

7 Chamanfar A, Jahazi M, Gholipour J *et al*. *Materials Science & Engineering A*[J], 2012, 555: 117

8 Li W Y, Vairis A, Preuss M *et al*. *International Materials Reviews* [J], 2016, 61(2): 71

9 Kelly Matthew R, Schmid Steven R, Adams Daniel C *et al*. *Journal of Manufacturing Processes*[J], 2019, 39: 26

10 McAndrew A R, Colegrove P A, Bühr C *et al*. *Progress in Materials Science*[J], 2018, 92: 225

11 Bhamji I, Preuss M, Threadgill P L *et al*. *Materials Science & Engineering A*[J], 2010, 528: 680

12 Buff G, Cammalleri M, Campanell D *et al*. *Materials & Design* [J], 2015, 82: 238

13 Mogami H, Matsuda T, Sano T *et al*. *Materials & Design*[J], 2018, 139: 457

14 Bhamji I, Moat R J, Preuss M *et al*. *Science & Technology of Welding & Joining*[J], 2012, 17(4): 314

15 Geng P H, Qin G L, Zhou J *et al*. *International Journal of Mechanical Sciences*[J], 2019, 152: 420

16 Ma T J, Chen X, Li W Y *et al*. *Materials & Design*[J], 2016, 89: 85

17 Wang X Y, Li W Y, Ma T J *et al*. *Materials & Design*[J], 2017, 116: 115

18 Vairis A, Frost M. *Materials Science & Engineering A*[J], 2000, 292(1): 8

19 Vairis A, Frost M. *Wear*[J], 1998, 217: 117

20 Wang X Y, Li W Y, Ma T J *et al*. *Materials Science & Engineering A*[J], 2019, 743: 12

21 Threadgill P L. *Materials Science & Engineering A*[J], 1995, 192-193(2): 640

22 Lee W B, Kim Y J, Jung S B. *Intermetallics*[J], 2004, 12: 671

23 Dong H G, Yu L Z, Gao H M *et al*. *Transactions of Nonferrous Metals Society of China*[J], 2014, 24: 3126

24 Dong H G, Yu L Z, Deng D W *et al*. *Advanced Manufacturing Processes*[J], 2014, 30(9): 1104

25 Wang L, Liu Y, Zhang W *et al*. *Intermetallics*[J], 2011, 19: 68

26 Dalgaard E, Wanjara P, Gholipour J *et al*. *Acta Materialia*[J], 2012, 60: 770

27 Schwaighofer E, Clemens H, Mayer S *et al*. *Intermetallics*[J], 2014, 44: 128

28 Dey S R, Hazotte A, Bouzy E. *Intermetallics*[J], 2009, 17: 1052

29 McAndrew A R, Colegrove P A, Addison A C *et al*. *Materials & Design*[J], 2015, 66: 183

30 Wang G, Xu L, Cui Y Y *et al*. *Acta Metallurgica Sinica*[J], 2016, 52(9): 1079 (in Chinese)

31 Li W Y, Ma T J, Li J L. *Materials & Design*[J], 2010, 31: 1497

32 Chen G Q, Zhang B G, Liu W *et al*. *Intermetallics*[J], 2011, 19: 1857

在线去应力退火对线性摩擦焊TiAl合金接头微结构与力学性能的影响机制

陈　曦[1]，张　钊[1]，谢发勤[1]，马铁军[2]，李文亚[2]，吴向清[1]

(1. 西北工业大学 民航学院，陕西 西安 710072)

(2. 西北工业大学 材料学院 陕西省摩擦焊接工程技术重点实验室 凝固技术国家重点实验室，陕西 西安 710072)

摘　要：采用在线去应力退火工艺对线性摩擦焊TiAl合金接头进行处理，避免了焊后裂纹的产生。显微组织分析表明，接头焊缝区与热力影响区界限明显，焊缝区主要由等轴γ晶组成，并含有少量的α_2相。靠近焊缝的热影响区内的层状γ晶具有明显的流线特征，其方向与焊接界面热塑性金属的流动方向一致。接头的显微硬度从母材区到焊缝区呈逐渐增加的趋势，焊缝区显微硬度相较于母材区增加了约1700 MPa；接头的室温抗拉强度与母材相当，在683 MPa到717 MPa之间。焊缝区的细晶强化效应是接头强度较高的主要原因。

关键词：线性摩擦焊；TiAl合金；在线去应力退火；显微组织；力学性能

作者简介：陈　曦，男，1988年生，博士，助理教授，西北工业大学民航学院，陕西 西安 710072，电话：029-88460937，E-mail：chenxb@nwpu.edu.cn